ALLEN INSTITUTE for BRAIN SCIENCE

Allen Cell Types Database

TECHNICAL WHITE PAPER:
GLIF MODELS

OVERVIEW

Generation of detailed biophysical data through standardized, systematic experimental methods facilitates the creation of computational models that simulate or predict cell behavior. The data created as part of the Allen Cell Types Database can be used in multiple different types of models and simulations. For simulations of neural networks, there is a tradeoff between the size of the network that can be simulated and the complexity of the model used for the individual neurons. A series of models of increasing complexity was constructed to reproduce the spiking behaviors of the recorded mouse and human neurons. Starting with a leaky integrate-and-fire model, three generalizations were added: a) after-spike currents which represent the slower effects of ion channels activated by an action potential, b) subthreshold voltage and spike-dependent changes in threshold caused by the activation and inactivation of ion channels and c) voltage and threshold reset rules derived, from the electrophysiology data. These rules determine how the threshold and voltage are reset after a spike and depend on the state prior to the action potential. Electrophysiological stimuli were specifically designed to estimate some of the parameters of the generalizations. Following these initial estimates, a threshold parameter was further tuned to optimize the reproduced spike times generated by a training noise stimulus. The optimization method was based on maximizing the likelihood of a model neuron with intrinsic noise exactly reproducing the spike train observed in the experiment. The model performance was subsequently evaluated on a test stimulus: for different time scales, the fraction of the variance of the neuronal response which was explained by the model was computed.

To explore the level of model complexity needed to describe the firing behavior of neurons, linear models were created with increasing levels of complexity. Standard leaky integrate-and-fire (LIF) models were the starting point, followed by progression to more generalized leaky integrate-and-fire (GLIF) models. In this Technical White Paper, models of different levels of complexity are defined. Then, the stimuli necessary for model creation are described. Next, methods for extracting model parameters from the electrophysiology data are discussed. After this, a description of the post-hoc optimization process and error functions by which threshold is additionally tuned is provided. Finally, metrics for evaluation of how well the models reproduce the spike times of the neurons are described.

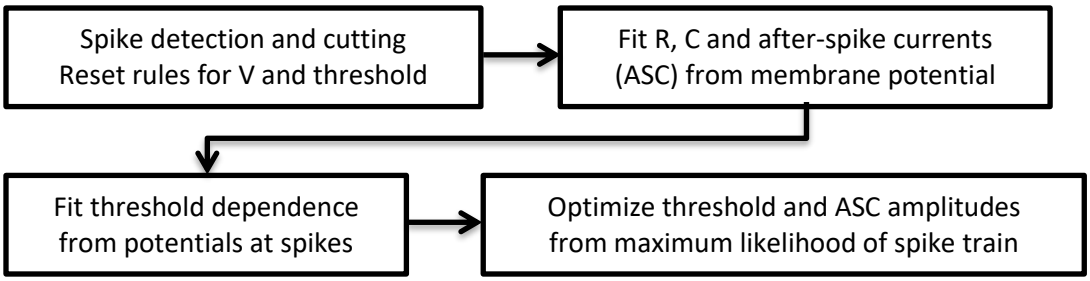

Figure 1. Flow chart for the primary components of the parameter fitting.
The structure is similar to those used in previous studies (Mensi *et al.* 2011).

MODEL DEFINITIONS

Below the five different GLIF models are defined in order of increasing level of complexity. **Figure 2** illustrates the iterations between the state variables in the model equations. **Figure 8** shows the progression of models for two neurons.

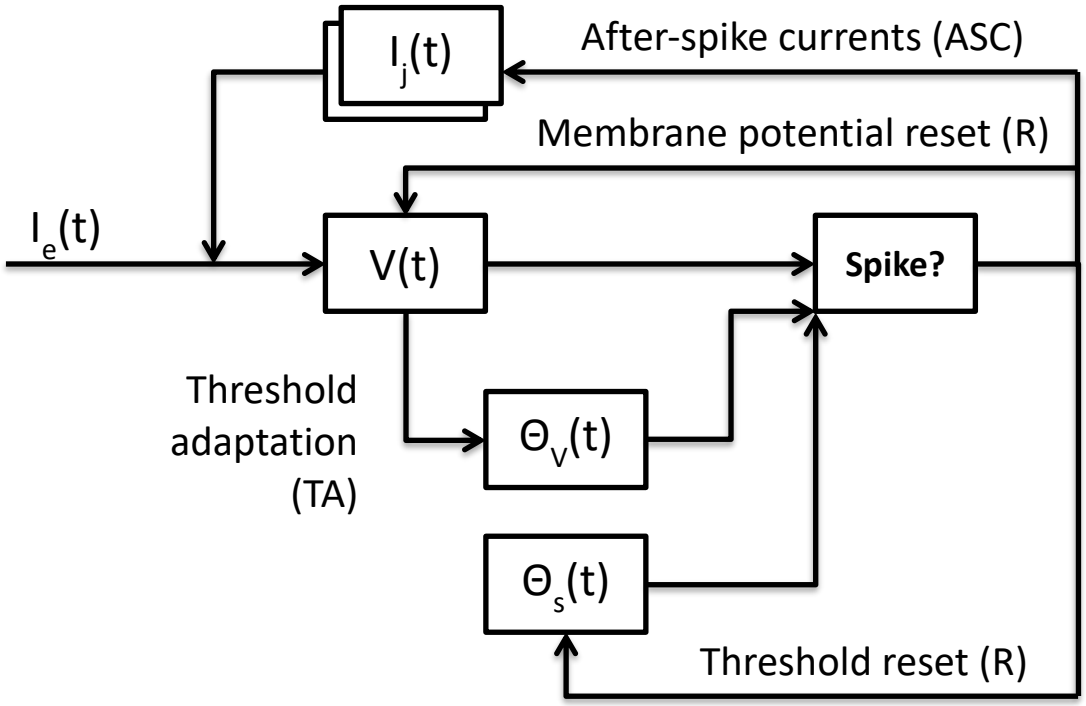

Figure 2. Interactions between state variables for different levels.

Leaky Integrate-and-Fire ($GLIF_1$:LIF)

The leaky integrate-and-fire (LIF) neuron was a hybrid system characterized by

1. An evolution equation for the membrane potential $V(t)$ (which is the only state variable in this case) as a function of the neuron's capacitance (C), membrane conductance (G), resting potential (E_L), and the time dependent external current (I_e):

$$V'(t) = \frac{1}{C}\left(I_e(t) - G\left(V(t) - E_L\right)\right)$$

,

2. A reset rule if the membrane potential becomes larger than a threshold $V(t) > \Theta_\infty$

$$V(t) \leftarrow V_r$$

Leaky Integrate-and-Fire with Biologically Defined Reset Rules (GLIF$_2$:LIF-R)

LIF-R had evolution equations for two state variables: the membrane potential $V(t)$ and a threshold $\Theta_s(t)$ which was updated by spikes and decays back to zero with a temporal constant b_s

$$V'(t) = \frac{1}{C}\left(I_e(t) - G\left(V(t) - E_L\right)\right)$$
$$\Theta_s'(t) = -b_s\Theta_s(t)$$

,

along with a reset rule if the membrane potential becomes larger than a threshold, which has both a constant (Θ_∞) and a spike-induced ($\Theta_s(t)$) component: $V(t) > \Theta_\infty + \Theta_s(t)$

$$V(t_+) \leftarrow E_L + f_v \times (V(t_-) - E_L) - \delta V$$
$$\Theta_s(t_+) \leftarrow \Theta_s(t_-) + \delta\Theta_s$$

The update to the spike-dependent component of the threshold is additive with a $\delta\Theta_s$ added after every spike. The update to the membrane potential has multiplicative coefficient f_v, and an additive one δV.

Leaky Integrate-and-Fire with After-spike Currents (GLIF$_3$:LIF-ASC)

In LIF models, the rapid membrane potential fluctuations due to the fast voltage-activated (*i.e.* sodium and potassium) ion channels during a spike were ignored. However, the ion channels activated by a spike could have effects over longer time scales. As the sharp membrane potential transitions during an action potential were stereotypical, the longer term effects were modeled as additional currents, which had predefined time scales (k_j), a multiplicative constant (R_j) which is typically set to 1, and an additive constant (A_j) to each current following a spike.

$$I_j'(t) = -k_j I_j(t);\ j = 1, ..., N$$
$$V'(t) = \frac{1}{C}\left(I_e + \sum_j I_j(t) - G\left(V(t) - E_L\right)\right)$$

The update rule, which applies if $V(t) > \Theta_\infty$, changes the

$$I_j(t_+) \leftarrow R_j \times I_j(t_-) + A_j$$
$$V(t_+) \leftarrow V_r$$

Leaky Integrate-and-Fire with Biologically Defined Reset Rules and After-spike Currents (GLIF$_4$:LIF-R-ASC)

Integrating the biological reset rules with the after-spike currents (described above) led to a model defined by:

$$I_j'(t) = -k_j I_j(t);\ j = 1, ..., N$$
$$V'(t) = \frac{1}{C}\left(I_e(t) + \sum_j I_j(t) - G\left(V(t) - E_L\right)\right)$$
$$\Theta_s'(t) = -b_s\Theta_s(t)$$

The update rule, which applies if $V(t) > \Theta_\infty + \Theta_s(t)$,

$$I_j(t_+) \leftarrow f_j \times I_j(t_-) + \delta I_j$$
$$V(t_+) \leftarrow E_L + f_v \times (V(t_-) - E_L) - \delta V$$
$$\Theta_s(t_+) \leftarrow \Theta_s(t_-) + \delta\Theta_s$$

Leaky Integrate-and-Fire with Voltage Dependent Threshold, Biologically Defined Reset Rules, and After-spike Currents (GLIF$_5$:LIF-R-ASC-AT)

Generalized leaky integrate-and-fire (GLIF) neurons were a hybrid system characterized by an evolution equation for the state variables and a reset rule if a spike occurred. For the LIF-R-ASC-AT, the state variables were the membrane potential $V(t)$, a set of after-spike currents $I_j(t)$, and a threshold which had spike (Θ_s) and membrane potential (Θ_v) dependent components. It was assumed that these state variables evolved in a linear manner between spikes:

$$I_j'(t) = -k_j I_j(t);\ j = 1, ..., N$$
$$V'(t) = \frac{1}{C}\left(I_e(t) + \sum_j I_j(t) - G\left(V(t) - E_L\right)\right)$$
$$\Theta_s'(t) = -b_s\Theta_s(t)$$
$$\Theta_v'(t) = a(V(t) - E_L) - b_v(\Theta_v(t) - \Theta_\infty)$$

Where C represented the neuron's capacitance, *G* the membrane conductance, E_L the resting membrane potential, I_e the external current, k_i the time constants of the after-spike currents, b_s and b_v the time constants of the spike- and voltage-dependent components of the threshold, and *a* the voltage dependence of the threshold.

A spike was generated if $V(t) > \Theta_v(t) + \Theta_s(t)$, and the state variables were updated according to the reset rules:

$$I_j(t_+) \leftarrow f_j \times I_j(t_-) + \delta I_j$$
$$V(t_+) \leftarrow E_L + f_v \times (V(t_-) - E_L) - \delta V$$
$$\Theta_s(t_+) \leftarrow \Theta_s(t_+) + \delta\Theta_s$$
$$\Theta_v(t_+) \leftarrow \Theta_v(t_-)$$

where the value immediately after the spike, (t_+) was related to the value immediately before the spike (t_-) via a set of update parameters: *f* represented the fraction of the prespike value of a variable which was maintained after the spike, and *δ* represented the values updated by a spike.

PARAMETER FITTING

Criteria for Model Creation

For a GLIF model to be created, a base set of stimuli (referred to as "sweeps") had to pass quality control (QC). For a model of any level to be created, the following sweeps had to pass QC:

- One subthreshold long square (in order to estimate Maximum Likelihood Based on Internal Noise (MLIN) optimization parameters)

- One subthreshold short square (to estimate threshold)
- One suprathreshold short square (to estimate threshold)
- Two noise 1 (training)
- Two noise 2 (testing)

In addition, for any model requiring reset rules (*i.e.*, LIF-R, LIF-R-ASC or A LIF-R-ASC-AT), a set of triple short square sweeps had to be available. For a description of these stimuli, see the **Electrophysiology Overview** in the Documentation tab. The noise stimuli were required for model optimization and testing, while the other stimuli were needed for parameter extraction as described below. Only sweeps that passed QC were used in either preprocessing or optimization.

Data Preprocessing
Before parameter fitting, there was a preprocessing stage with the primary goal of calculating basic properties of the electrophysiological data (such as the resting potential and spike times) and removing the rapidly varying potential that occurs during a spike.

Resting potential [E_L]: The resting potential was defined as the mean resting potential of the noise 1 sweeps as calculated in the **Electrophysiology Overview** in the Documentation tab (averaging the pre-stimulus membrane potential).

Spike initiation detection: For a detailed description of how spikes were detected please see the Action Potential Identification section of the **Electrophysiology Overview** in the Documentation tab.

Spike cutting: The sections of the voltage traces influenced by the highly non-linear ion fluctuations during the action potential were not included in the fitting of the subthreshold elements. The duration of the spike, which was removed from the trace, was calculated by aligning all of the action potentials of noise 1 to the spike initiation (**Figure 3**). Then a linear dependence was fit between the voltage at spike initiation (prespike voltage) and the voltages at each time point in a window of 1 to 10 ms after spike initiation (postspike voltages). The duration of the spike was then chosen by considering the linear fit of each prespike and postspike combination. The fit which minimized the residuals was chosen to define the spike duration and voltage reset rules described below (**Figure 4**).

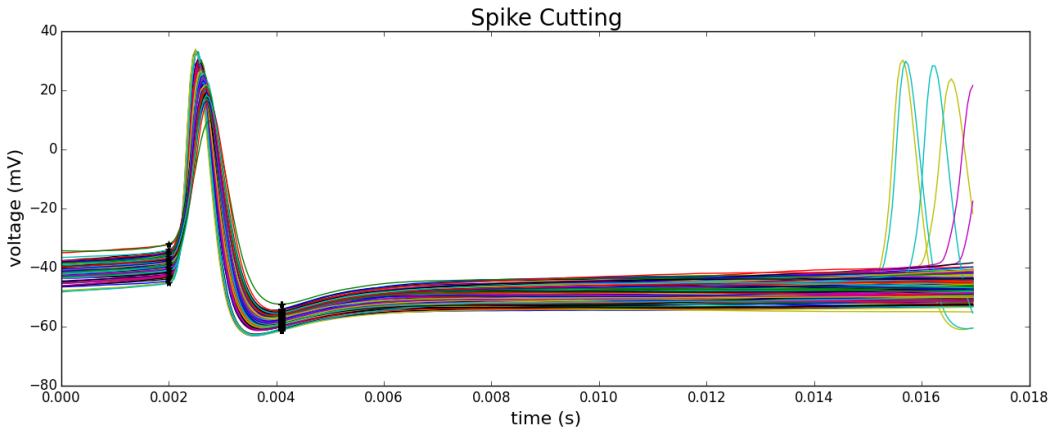

Figure 3. Spike cutting.
The action potentials are excluded from model fitting. All spikes from the noise 1 stimuli are aligned. Dots represent spike initiation and termination found by minimizing the residuals from a linear regression **between prespike voltage and postspike voltage in a window 1 to 10 ms after spike initiation.**

Voltage reset rules [$V(t_+)$]: When the model spiked, the voltage was reset according to rules that depended on the model type. In the LIF and LIF-ASC models, the voltage was reset to the resting potential. For the LIF-R, LIF-R-ASC, and LIF-R-ASC-AT models, the postspike voltage was reset via rules extracted from the electrophysiological traces during the spike cutting calculation described above. The voltage of the model was

reset by V_{ma} = slope*V_{mb} + intercept, where V_{mb} was the voltage of the model before the spike and V_{ma} was the voltage of the model after the spike (**Figure 4**). The intercept and slope were calculated via the linear regression fit to the prespike voltage and postspike voltages explained in the *Spike Cutting* section above.

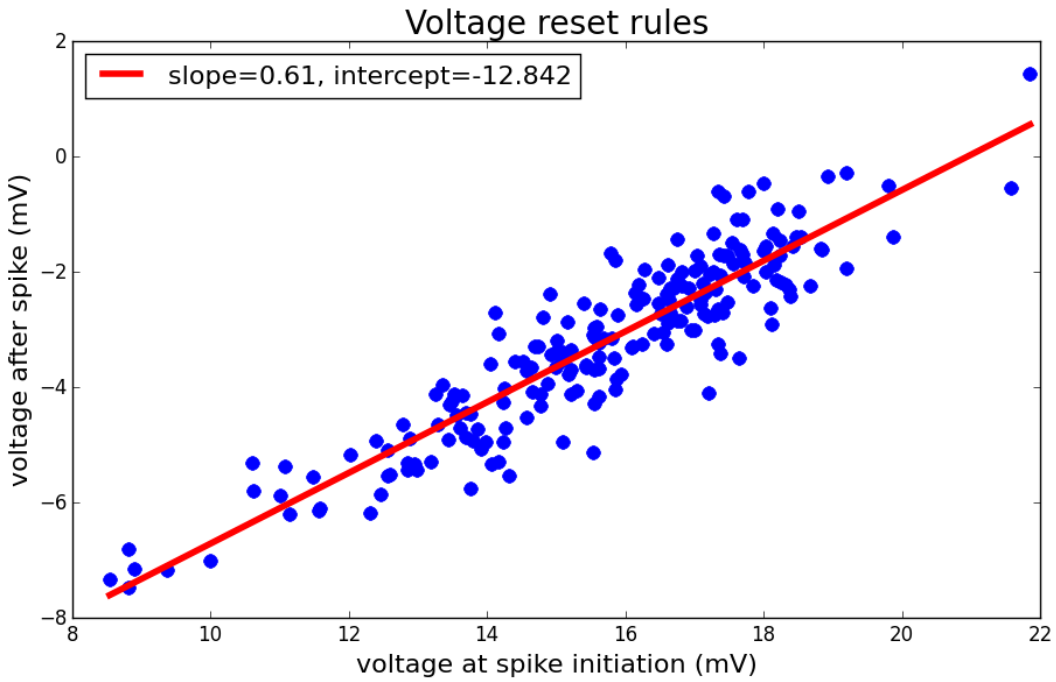

Figure 4. Reset rules were found by fitting a line between the voltage at spike initiation and the voltage at spike termination.
In the LIF-R, LIF-R-ASC, and LIF-R-ASC-AT models, voltage reset is calculated by inserting the model voltage when it reaches threshold into the equation defined by the line. Note that the axes on this plot are converted into the model frame of reference by subtracting the resting potential and the prespike non-linearity correction. This correction is applied to the voltage reset rules.

Parameter Fitting

All fitting (and optimization) requiring noise stimuli were performed on the training noise set (noise 1). The holdout noise stimuli (noise 2) were reserved for testing to protect against "overfitting". Descriptions of the specific fitting calculations follow. Brackets denote the variable notation in the model equation section above.

Capacitance [C] and Resistance [1/G]: Capacitance and resistance were calculated via a linear regression of the subthreshold noise in the first epoch of noise stimulation within the three-epoch noise sweeps (this stimulus did not elicit any spikes).

After Spike Currents: The membrane potential for a leaky integrate-and-fire neuron with after-spike currents I_j(t) evolved according to the equations outlined first under the LIF-ASC section.

For all of the GLIF model levels where after-spike currents were included (LIF-ASC, LIF-R-ASC, and LIF-R-ASC-AT), after spike currents were modeled using exponential decaying basis functions with an amplitude and a time scale. The time scales and amplitudes were obtained by providing two from a set of five exponential decaying basis currents with varied time scales ($1/k_j$) ([3.33, 10, 33.3, 100, 333.33] ms) to a generalized linear model (GLM). The GLM was used to calculate the resistance and amplitudes corresponding to each basis current by regressing the sum of the derivative of the voltage, the external current divided by the capacitance and the leak current ($dV/dt + I_e/C$) against the basis currents and leak term. *C*, and *EL* were calculated as mentioned in the above text. The GLM was run with all combinations of two of the five possible time scales leading to a choice among (${}^5C_2 = 10$) pairs of basis currents. The optimal pair of basis currents chosen was the one which resulted in the maximum log-likelihood value.

The basis currents, with their respective amplitudes, were summed together to obtain the total effective after-spike current. To ensure that the GLM estimates were not affected by the very large currents present during a spike, the regression was always performed using the voltage trace with the spikes removed as mentioned in the Spike Cutting section above.

Instantaneous threshold [Θ_∞]: The model neuron spiked when the voltage of the model crossed the threshold of the model. An estimate for the instantaneous threshold was the voltage at spike initiation of the lowest amplitude suprathreshold short square. This was an essential parameter, and it was tuned in the post-hoc optimization of every model.

Spike component of the threshold [Θ_s]: The evolution of the threshold of LIF-R, LIF-R-ASC, LIF-R-ASC-AT contains a "spiking component" of the threshold. This contribution to the threshold represented the effect spiking had on the threshold of the neuron due to inactivation of voltage-dependent sodium channels. The inactivation could be interpreted as a rise in the threshold of the neuron, and the movement from the inactive to a closed state could be modeled as a linear dynamical process. The change in threshold was fit with an exponential, and the values of its amplitude and time constant were calculated from the triple short square sweep set data (**Figure**). For each blip in the triple short square data that produced a spike, the voltage at spike initiation (the threshold) was calculated. In this case, the mean of the threshold of the first spike was taken to be the triple short square instantaneous threshold. For all spikes that were not "first spikes," the time since the last spike was calculated (referred to as an ISI). An exponential was then fit to the ISI versus threshold data (**Figure 5**). The exponential was forced to decay to the value of the triple short square instantaneous threshold (the threshold of the first spike in each short square triple).

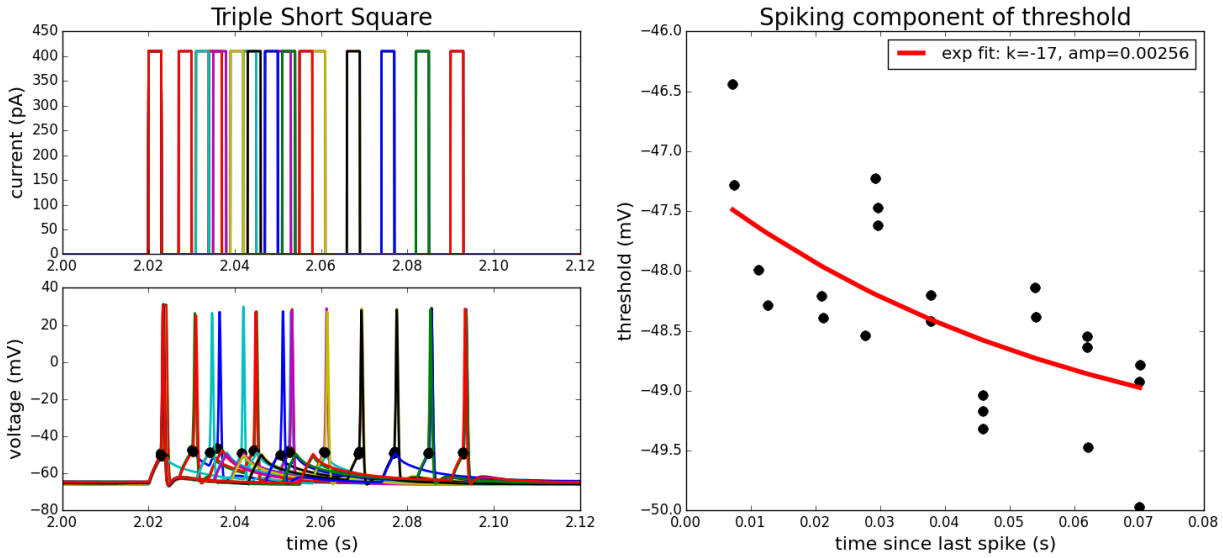

Figure 5. The spiking component of the threshold is defined by an exponential function fit to the time between spikes and the voltage at spike initiation of the triple short square data set.
Different colors in data represent different sweeps. Black dots denote spike initiation.

Subthreshold voltage component of the threshold [Θ_V]: LIF-R-ASC-AT contained both a "spiking" component of the threshold (see above) and a "subthreshold voltage" component of the threshold. The subthreshold voltage component represented the effect of subthreshold membrane potential on the threshold (*e.g.*, voltage dependence of sodium channel reactivation). The voltage component of the threshold evolved according to the last equation under LIF-R-ASC-AT.

The exact solution for the above evolution equation was then used to obtain initial estimates for the parameters a_v and b_v using a Nelder-Mead simplex optimization.

Post-Hoc Optimization

After the parameters were extracted from the electrophysiological data as described in the "Iterative Parameter Fitting" section, an optimization step was performed. During optimization, the instantaneous threshold was optimized using a Nelder-Mead simplex algorithm (Python scipy module scipy.optimize.fmin). **Figure 9** shows the rastergrams of optimized models for two neurons.

Forced-spike Model Paradigm

During optimization, each spike should be fit without erroneous after-spike current history affecting the fitting of the subsequent spikes. Therefore, the model was forced to spike at the times the neuron spikes (**Figure 6**). The model continued to run regardless of whether or not the voltage of the model crossed the threshold of the model. The model voltage, threshold, and after-spike amplitudes were forced to reset at the time the neuron spiked. The reset rules were denoted in the GLIF model section above. When a model was run in its normal forward-running manner, the prespike values of the voltage, $V(t_-)$, threshold, $\Theta(t_-)$, and AS currents, $I_j(t_-)$, were the values of the model at the point where the model voltage crossed the model threshold. In the forced spike paradigm, to ensure that the voltage model was reset below the threshold of the model, the prespike voltage was set equal to the prespike threshold, $V(t_-) = \Theta(t_-)$ at the time of the neuron spike. Note that this reset only affected LIF-R, LIF-R-ASC, LIF-R-ASC-AT, where the prespike voltage affected the postspike voltage.

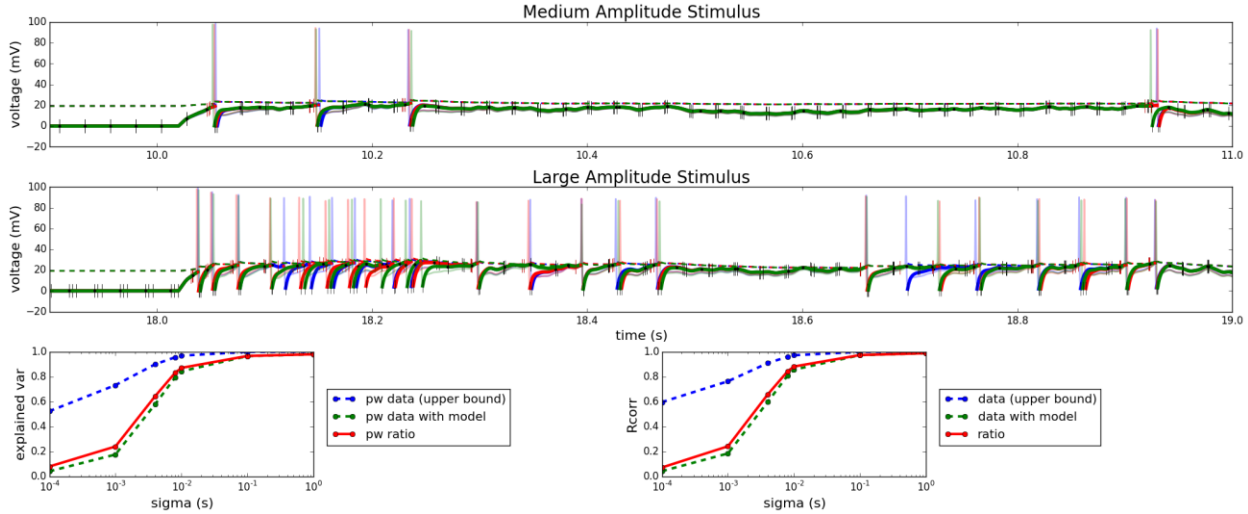

Figure 6. The MLIN function is evaluated during a forced-spike model paradigm.
Translucent colored lines are neuron voltage traces from several repeats of the same stimuli. Solid colored lines are corresponding model traces forced to spike at the time of the biological data. Dashed lines are model thresholds. Black tick marks denote non-spike bins specified in the MLIN optimization function. Red tick marks denote spike bins. The dots represent the location within the bin where the voltage difference between the model voltage and model threshold was minimized. Note that the model was run with a resting potential set equal to zero. Here the data traces are shifted so that their resting potential has a mean equal to zero.

Objective Function: Maximum Likelihood Based on Internal Noise (MLIN)

Similar to a series of previous studies (Paninski, Pillow, Simoncelli, 2004; Dong *et al*. 2011; Mensi *et al*. 2012; Pozzorini *et al*. 2013), the likelihood that the observed spike train was obtained by the model was maximized. However, the exact method of constructing the likelihood was different in that the noise is not tuned but rather uses a direct estimate of the biological neuron's internal noise (Maximum Likelihood based on Internal Noise) was used.

Because these GLIF models were deterministic, estimating the likelihood required adding a source of noise external to the model. Rather than searching for the parameters of this noise, a parametric description of the internal noise of each neuron was used (**Figure 7**). As this internal noise could depend on the membrane potential, and the most relevant potential was near threshold, the variation in membrane potential during the steady state period of the largest subthreshold square pulse response was characterized.

The probability density of the neuron being at a potential *v* away from its mean was fit with an exponentially decaying function (denoted by “expsymm” in **Figure 7**):

$$p(v) = \frac{1}{2\delta v} exp(-\frac{|v|}{\delta v})$$

This variation was considered to be additive to the membrane potential of the deterministic neuron. This allowed the computation of the probability that a neuron with the given noise would produce a spike if the deterministic model had a difference between threshold and membrane potential:

$$\Delta V(t) = \Theta(t) - V(t) = \Theta_s(t) + \Theta_v(t) + \Theta_\infty - V(t)$$

$$p_{spike}(t) = \int_{\Delta V(t)}^{\infty} p(v)dv = \int_{\Delta V(t)}^{\infty} \frac{1}{2\delta v} exp(-\frac{|v|}{\delta v})dv = 1 - c(\Delta V(t))$$

where *c* represented the cumulative distribution of the intrinsic noise.

The likelihood of the model producing a set of spikes at the times the biological neuron produces them was:

$$p_{spikes} = \prod_{t \in t_s} p_{spike}(t)$$

However, the model neuron must both produce spikes when the biological neuron does, and not produce spikes when the biological neuron does not.

The likelihood of a model neuron not producing spikes was not independent for two nearby time points, as the intrinsic noise had a nontrivial autocorrelation. To estimate the likelihood of the model neuron not producing spikes at the times the biological neuron does not produce spikes, one sample for the internal noise was drawn for each time period of the autocorrelation, and following this time scale a new independent sample was drawn. As such, the inter-spike intervals were binned with bin sizes equal to the autocorrelation (typical autocorrelations time scales were much smaller than the inter-spike intervals (**Figure 7**)). The grid times started from a spike time and advanced by the autocorrelation time scale, ending at a predefined short time (5 ms) before the next spike. To estimate the likelihood of a neuron not producing a spike within a bin, the minimal difference between threshold and membrane potential within the bin was chosen, which generated the grid differences:

$$p_{nospikes} = \prod_{t \in t_{grid}} c(\Delta V_{grid})$$

The log likelihood of the entire spike train being exactly reproduces was

$$LLIN = Log\left(p_{spikes} p_{nospikes}\right) = \sum_{t \in t_s} (1 - c(\Delta V(t))) + \sum_{t \in t_{grid}} c(\Delta V_{grid})$$

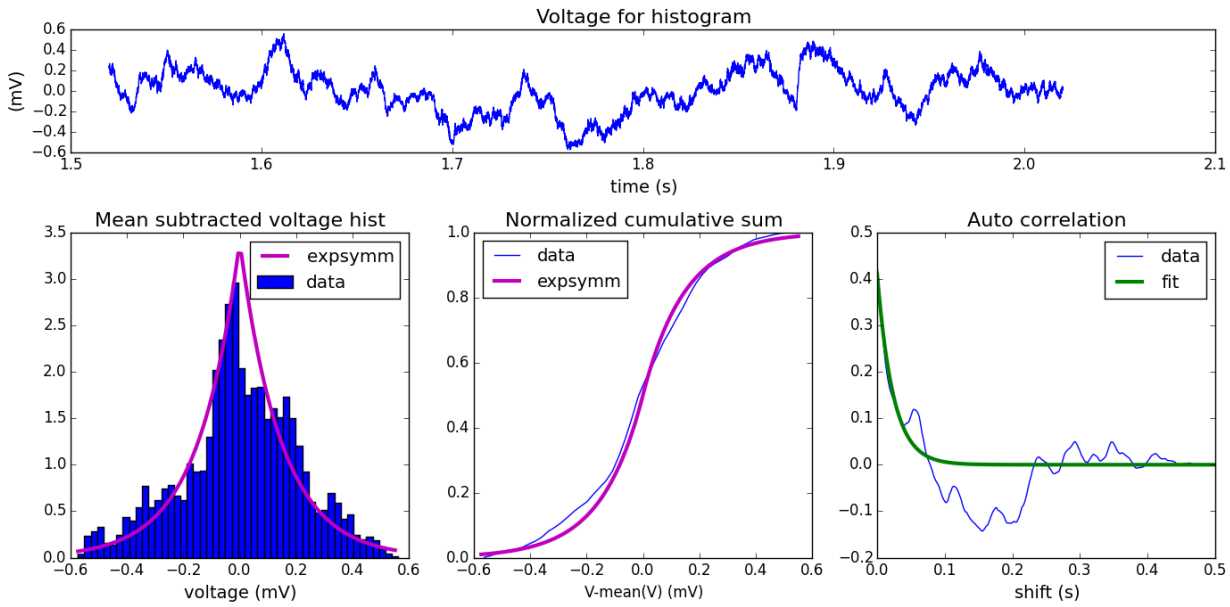

Figure 7. Parameters of the MLIN objective function were extracted from the data.
A distribution of voltages is created from the tailing end of the largest amplitude subthreshold square pulse available (top panel). This distribution is then fit by a symmetrically decaying exponential function denoted as expymm in the plot legends. The width of the non-spiking bins is chosen via a fit of the autocorrelation.

Simplex

Parameters were optimized to minimize MLIN using a simplex algorithm (Nelder-Mead). To optimize normalized parameters, the parameters of instantaneous threshold and after-spike amplitudes themselves were not optimized. Instead, the parameters remained at the values provided by the preprocessor, and multiplicative factors (coefficients) of these parameters were optimized.

To ensure that the optimization routine did not return a sub-optimal local minimum, the overall optimization was rerun three times. Each time the overall optimization was rerun, the coefficients were randomly perturbed between an interval of +/- 0.3 of their last found optimized value. Within each of the overall reruns, the stability of the convergence was confirmed by reinitializing the algorithm (*i.e.* re-inflating the simplex) three times at the optimal position in parameter space with a small random perturbation within an interval of +/- 0.01 and then re-running the simplex.

Because the voltage dynamics were governed by a first-order linear differential equation, the voltage dynamics were forward simulated over a single time step using an exact Euler time stepping method. The timestep was chosen to be 0.2 ms. The current that forces the dynamics was averaged across the timestep.

MODEL EVALUATION OF SPIKE TIMES

After all parameters of the model were optimized, the activity of the models was determined using an Euler exact method. The spike times of the model were evaluated against the spike times of the neuron. Two metrics were used to evaluate how well the models do at reproducing the spike times of the neuron. The first was a widely used correlation-based method published by Schreiber *et al*. 2003. The second metric (used on the website) was the explained temporal variance described below (**Figure 6**), which similarly to the reliability focused on how well the temporal dynamic of the response is captured by the model, but it has a value of 0 if the model is at chance.

A spike train, ST, was represented as a time series of binary numbers. All numbers in the ST were zero unless a spike occurred: a spike was denoted with a one. Any spike train could be converted into a single train peristimulus time histogram, stPSTH by convolving a ST with a Gaussian.

In the case where there were many repeats of the same stimulus, a peristimulus time histogram (PSTH) could be calculated by taking the mean of the stPSTH at each instant in time. If there were *n* $stPSTH_i$ denoted with index *i,* where *i* goes from 1 to n, *i*=1,2...*n*, the PSTH was equal to the column mean of the $stPSTH_i$:

$$PSTH = \sum_{i}^{n} \frac{stPSTH_i}{n}$$

The variance in spiking output of neurons could be described by the variance of the PSTH. In general, the explained variance (EV) between any two PSTHs (multiple or single train) would be:

$$EV(PSTH_1, PSTH_2) = \frac{var(PSTH_1) + var(PSTH_2) - var(PSTH_1 - PSTH_2)}{var(PSTH_1) + var(PSTH_2)}$$

The explained temporal variance by the mean across-trials PSTH of the neuron EV_D would be an upper limit on how well the model could perform:

$$EV_D = mean_i \left(EV(stPSTH_{D_i}, PSTH_D)\right)$$

where *i* denotes the *i*th data stPSTH and *n* denotes the total number of data sweeps.

Since the models here were deterministic, the pairwise explained variance of the data with the model could be calculated by taking the mean of the explained variance between every data $stPSTH_D$ and the model $PSTH_M$.

$$pwEV_{DM} = mean_i \left(EV(stPSTH_{D_i}, PSTH_M)\right)$$

where *i* denotes the *i*th data stPSTH and *n* denotes the total number of data sweeps.

If the ratio of the *pwEV* of the model to the data versus the *pwEV* within the data was equal to 1, the model was performing maximally well. The ratio of the pairwise explained variance by the model to that by the multiple trial average was reported.

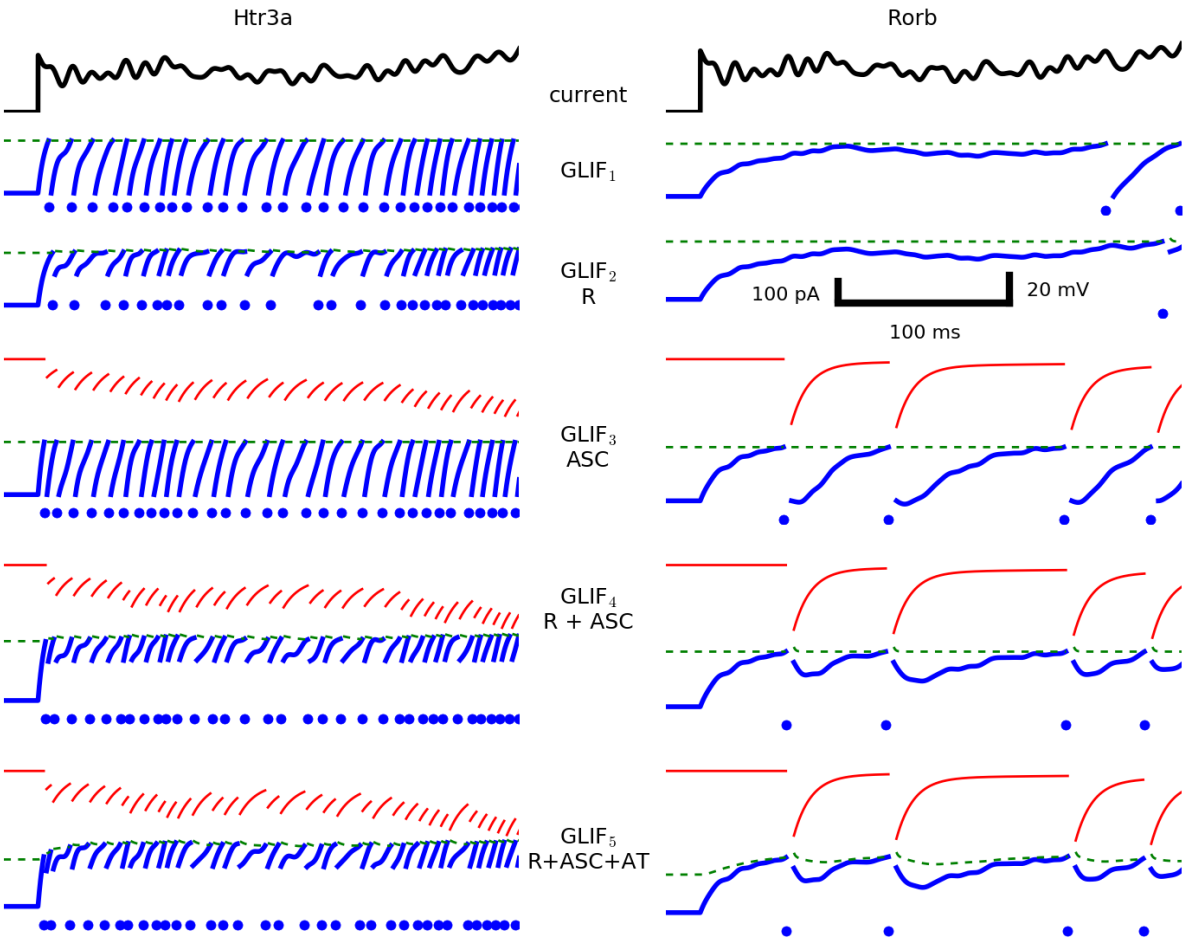

Figure 8. Illustration of the five GLIF models from two different transgenic lines (**Htr3a 477975366 and Rorb 314822529**). The injected current, $I_e(t)$, is plotted at the top in black. In all panels, the model trans-membrane potential, V(t), is pictured in blue (spike rasters are marked below), and the threshold, Theta, in dashed green. For models that contain afterspike currents, the total current is in red. The scale bar applies to all panels except to the injected current. $GLIF_1$: Equivalent to the standard LIF model, when V(t) reaches the constant threshold, a spike is produced. After a short refractory period, V is reset to a constant value. $GLIF_2$: The threshold Θ_s modestly increase with each spike, and decays to a constant. When V(t) reaches Theta s, the neuron spikes. After the refractory period, both V and Θ are reset to a value which is dependent on the state of the neuron before the spike. $GLIF_3$: Every action potential induces afterspike currents which decay back to zero. The level of induction depends on the state of the neuron before the spike. $GLIF_4$: Here, spike-induced changes in threshold and afterspike currents are combined and reset for all variables which are dependent on the state of the neuron before the spike. $GLIF_5$: The addition of a voltage-dependence to the threshold Θ.

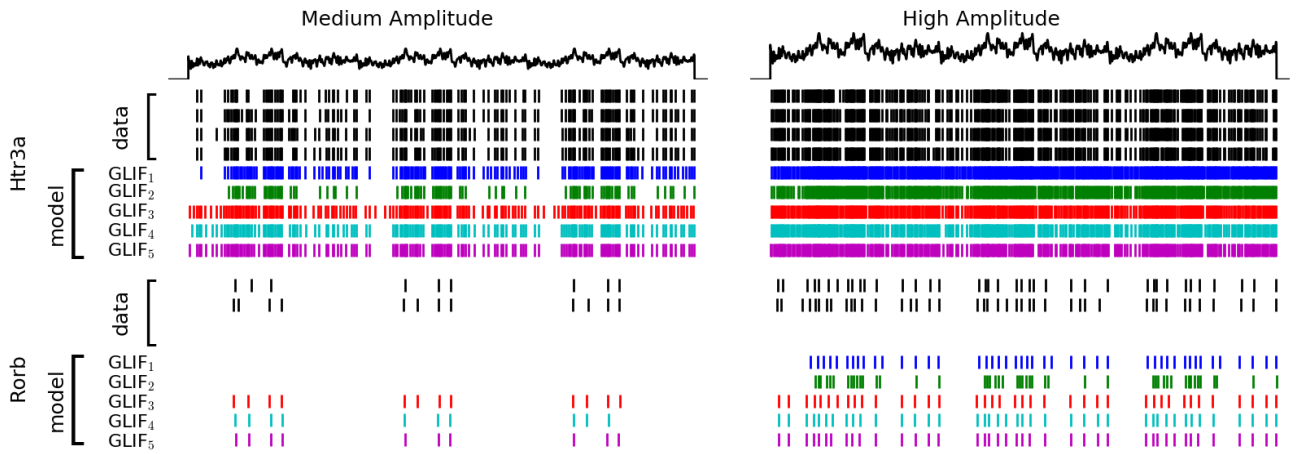

Figure 9. Rastergrams of biological data and all optimized model levels for 'hold out' test data for the two example cells: Htr3a 477975366 and Rorb 314822529. Injected current shown in black. Black rasters are spikes from recorded neurons to repeated current injections. Colored rasters correspond to the five different, deterministic models. The current injection is 3 s long. It is observed that as the $GLIF_1$ and $GLIF_2$ do not have a spike frequency adaptation mechanism, they have trouble reproducing simultaneously the firing patterns at multiple input amplitudes.

PYTHON VERSION

All code was implemented using python 2.7.8 via Anaconda 2.1.0 (64-bit) compiled with GCC 4.4.7 20120313 (Red Hat 4.4.7-1), Numpy version 1.9.0, Scipy version 0.14.0.

REFERENCES

Dong Y, Mihalas S, Russell A, Etienne-Cummings R, Niebur E (2011) Estimating parameters of generalized integrate-and-fire neurons from the maximum likelihood of spike trains. *Neural Computation* 23:2833-2867.

Mensi S, Naud R, Pozzorini C, Avermann M, Petersen CC, Gerstner W (2012) Parameter extraction and classification of three cortical neuron types reveals two distinct adaptation mechanisms. *Journal of Neurophysiology* 107:1756-1775.

Paninski L, Pillow JW, Simoncelli EP (2004) Maximum likelihood estimation of a stochastic integrate-and-fire neural encoding model. *Neural Computation* 16:2533-2561.

Pozzorini C, Naud R, Mensi S, Gerstner W (2013) Temporal whitening by power-law adaptation in neocortical neurons. *Nature Neuroscience* 16:942-948.

Schreiber S, Fellous JM, Whitmer D, Tiesinga P, Sejnowski TJ (2003) A new correlation-based measure of spike timing reliability. *Neurocomputing* 52-54:925-931.

APPENDIX

Table 1. State variables added by each mechanism.

Model	Symbol	Variable
LIF	$V(t)$	Membrane potential
ASC	$Ij(t)$	After-spike currents
R	$\Theta_s(t)$	Spike-dependent threshold component
TA	$\Theta_V(t)$	Voltage-dependent threshold component

The first level, LIF, contains only the membrane potential V(t). When history dependent reset rules are added in the second level LIF-R, the sate variables are V(t) and $\Theta_s(t)$. LIF-ASC adds afterspike currents, with the state variables V(t) and $I_j(t)$, and their combination, LIF-R-ASC has V(t), $\Theta_s(t)$ and $I_j(t)$. Adding the mechanisms which has a component of the threshold which is dependent on the membrane potential between spikes, LIF-R-ASC-TA leads to the state variables being V(t), $\Theta_s(t)$, $\Theta_V(t)$ and $I_j(t)$.

Table 2. Parameters added by each mechanism.

Model	Symbol	Parameter	Fit From	Post-hoc Optimized
LIF	C	Capacitance	V during low amplitude noise	No
LIF	G	Membrane conductance	Subthreshold V during noise	No
LIF	E_L	Resting potential	Resting V before noise	No
LIF	$\theta\infty$	Instantaneous threshold	Short square input	Yes
R	f_v	Voltage fraction following rest	All noise spikes	No
R	δV	Voltage addition following rest	All noise spikes	No
R	b_s	Spike-induced threshold time constant	Triple short square	No
R	$\delta\theta$	Threshold addition following reset	Triple short square	No
ASC	Aj	Afterspike current amplitudes	Subthreshold V during noise	Yes
ASC	k_j	Afterspike current time constants	Subthreshold V during noise	No
TA	a	Adaptation index of threshold	Prespike V during noise	No
TA	b_v	Voltage-induced threshold time constant	Prespike V during noise	No